JOURNAL OF PHYSICAL ORGANIC CHEMISTRY
*J. Phys. Org. Chem.* **12**, 635–644 (1999)

# Effect of substituents on the formation of isomeric isoxazolo heterocycles: rationalization by semi-empirical PM3 molecular orbital calculations

**Walter M. F. Fabian,[1]* Klaus Schweiger[2] and Robert Weis[2]**

[1]Institut für Organische Chemie, Karl-Franzens Universität Graz, Heinrichstr. 28, A-8010 Graz, Austria
[2]Institut für Pharmazeutische Chemie, Karl-Franzens Universität Graz, Universitätsplatz 1, A-8010 Graz, Austria

*Received 8 November 1998; revised 12 February 1999; accepted 19 February 1999*

**epoc**

ABSTRACT: The different behavior of 4-amino- *vs* 4-hydroxypyridinones **7** and **8**, respectively, towards hydroxylamine is rationalized with the aid of semi-empirical PM3 molecular orbital calculations including solvent effects. Four different mechanisms leading to either isoxazolo[4,3-*c*]pyridinones **9** or isoxazolo[4,5-*c*]pyridinones **10** are considered. Based on computed activation energies reaction of hydroxylamine via its oxygen atom as nucleophile is highly disfavored. For compound **7** a $\beta$-carbon addition of $NH_2OH$ at C-4 of the pyridinone accompanied by amine exchange and ring closure to **9** is by far the most feasible pathway. In contrast to **7**, according to both NMR spectroscopy and molecular orbital [semi-empirical PM3 and hybrid density functional/Hartree–Fock (B3LYP/6–31G*)] calculations, **8** exists as a mixture of tautomers **8A** (*ca* 20%) and (***Z***)-**8B** (*ca* 80%). Both tautomers of **8** are predicted to react with hydroxylamine at the hydroxyethylidene carbon atom [(***Z***)-**8B**] or acyl functionality (**8A**) to give hydroxyaminoethylidene compound **38** (oxime **23**). Subsequent cyclization of either of these intermediates leads to compound **10**. Copyright © 1999 John Wiley & Sons, Ltd.

KEYWORDS: Isomeric isoxazolo heterocycles; substituent effect; semi-empirical PM3 molecular orbital calculations

*Additional material for this paper is available from the epoc website at http://www.wiley.com/epoc*

## INTRODUCTION

Fused oxazolo and isoxazolo heterocycles show a wide variety of biological activity, ranging from antitumor to herbicidal properties.[1,2] Specifically, isoxazolo[4,5-*c*]pyridinones **1** (Scheme 1), available by reaction of 5-methylisoxazole-4-carboxamides,[3] exhibit hypolipidemic activity and are useful synthons for the preparation of hypnotics, muscle relaxants and tranquillizers.[3] An isomeric isoxazolo[4,3-*c*]pyridinone **2** has been synthesized by thermolysis of a 3-acetyl-4-azido-2(1*H*)-pyridinone.[4] Similarly, benzo-fused derivatives—important as precursors for herbicide analogues—have been obtained from 3-acyl-4-azido-2-quinolones.[5] 3-Acyl-4-hydroxyquinolones **3** can be aminated at the 3-acyl keto functionality by reaction with amines.[5a] It was expected that oxime **4** formed in the analogous reaction with hydroxylamine **11** could be cyclized to the isomeric isoxazolo[4,5-*c*]quinolones **5**. However, under the reaction conditions, by thermal Beckmann rearrangement, the corresponding oxazolo[5,4-*c*]quinolones **6** were obtained.[6] Recently, we have described a synthesis of both isomers of fused isoxazole derivatives with an interesting dependence of the preferred cyclization mode on the 4-substituent of the 3-acyl lactams **7** and **8**: 4-amino-substituted derivatives **7** preferentially yield isoxazolo[4,3-*c*]pyridinones **9**; in contrast, 4-hydroxy derivatives **8** lead to the formation of isoxazolo[4,5-*c*]pyridinones **10**.[7] Finally, it is worth mentioning that isoxazoles have proved as key intermediates in the synthesis of biologically active oxygen heterocyclic triones.[8]

Given the importance of this class of compounds and the general significance of reactions between electrophilic and nucleophilic centers for the synthesis of heterocycles,[9] we found it worthwhile to investigate this interesting influence of the substituent in position 4 of the heterocycle on the direction of the cyclization in more detail. In continuation of our previous work on computational studies on the reaction of carbonyl compounds with nucleophiles,[10] in this paper the results

**Correspondence to:* W. M. F. Fabian, Institut für Organische Chemie, Karl-Franzens Universität Graz, Heinrichstr. 28, A-8010 Graz, Austria.
E-mail: walter.fabian@kfunigraz.ac.at

 CCC 0894–3230/99/080635–10 $17.50

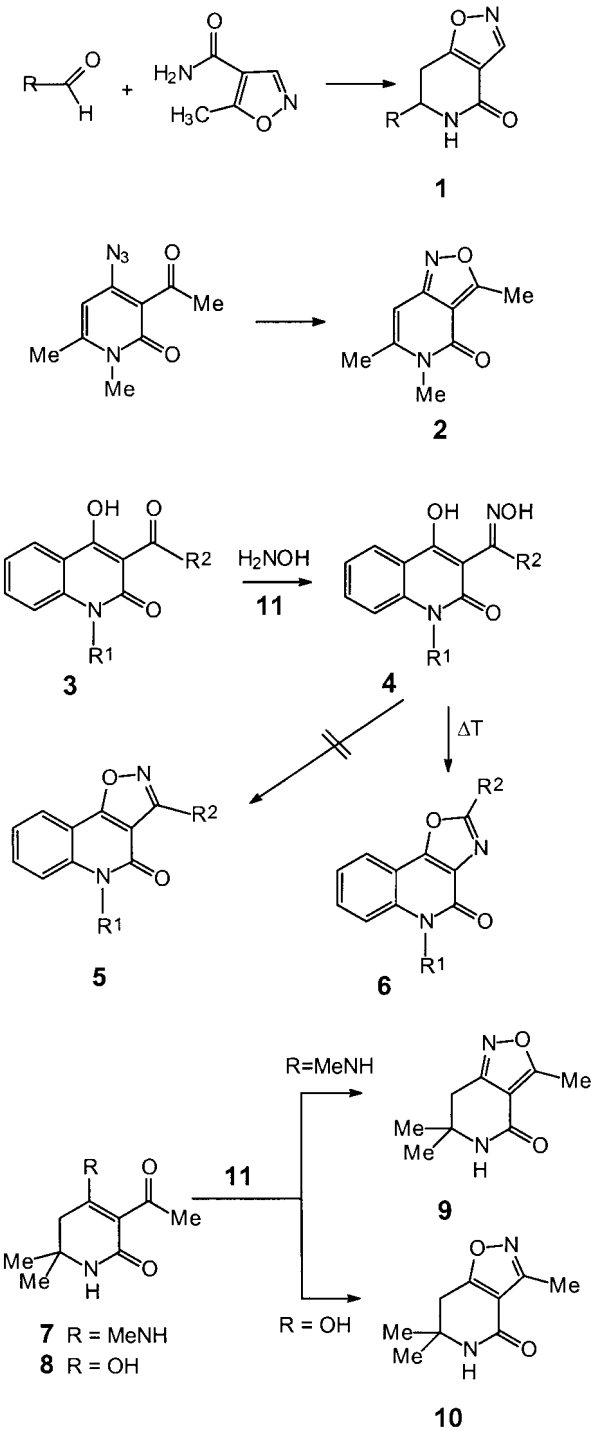


Scheme 1

of semi-empirical molecular orbital calculations on the reactions of **7** and **8** with hydroxylamine **11** to give either **9** or **10** are presented.

## CALCULATIONAL DETAILS

From previous experience[10] for reactions of this type, a complex behavior was expected. Hence it was not considered feasible to perform sufficiently sophisticated *ab initio* or density functional calculations (see below, however, for B3LYP/6–31G* calculations on the tautomers of **7** and **8**) for the systems under investigation and, especially, their complete reaction pathways. On the other hand, despite some shortcomings of semi-empirical methods, e.g. overestimation of the stability of tetrahedral intermediates, these methods have proved to give reasonable results for reactions of carbonyl compounds with nucleophiles. In particular, mechanistic details such as the identification of the rate-determining step or the influence of substituents on the kinetics could be successfully calculated[10] by the semi-empirical AM1 or PM3 method. Therefore, in the present investigation all calculations were performed by the semi-empirical PM3[11] method using the VAMP program.[12] Geometries were completely optimized (keyword PRECISE) by the eigenvector following routine.[13] Transition states were approximately located by reaction coordinate calculations, refined by gradient norm minimization and characterized by force constant calculations. In addition, downhill optimizations along both directions of the normal mode corresponding to the imaginary frequency (intrinsic reaction coordinate calculations, IRC) were done.

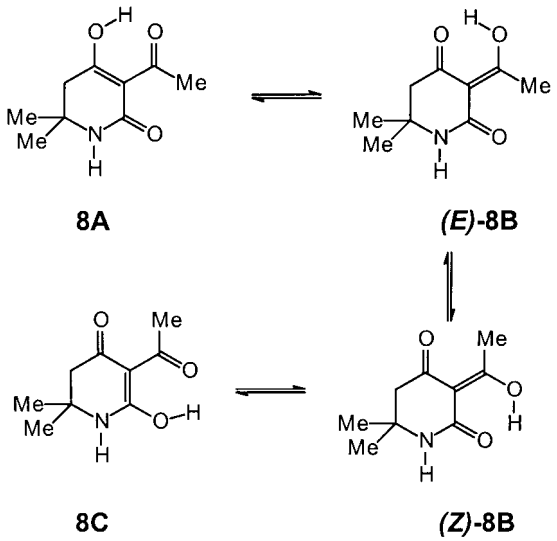


Scheme 2

Solvent effects ($H_2O$) were treated by the self-consistent reaction field approximation (based on Tomasi and co-workers' treatment of the reaction field[14a]) as implemented in the VAMP package.[14b] A vdW-shaped cavity with van der Waals radii scaled by 1.2 was employed.[15] The tautomers of compounds **7** and **8** (see Scheme 2) were also computed at the hybrid density functional/Hartree–Fock level of theory (B3LYP/6–31G*)[16] using the Gaussian 94 program suite.[17] Zero-point energies (ZPE) are unscaled. Bulk solvent effects (aqueous solution, $\varepsilon = 78.5$) were estimated by the self-consistent isodensity continuum model (SCIPCM)[18] with an isodensity surface cut-off of 0.0004 au.

**Table 1.** B3LYP/6–31G* –SCIPCM (including ZPE corrections, gas-phase values in parentheses) and PM3–SCRF computed energies (in kJ mol$^{-1}$) of tautomers **A**, **(*E*)-B, (*Z*)-B** and **C** for compounds **7** and **8**[a]

| | 7 | | 8 | |
|---|---|---|---|---|
| Tautomer | B3LYP/6–31G* | PM3 | B3LYP/6–31G* | PM3 |
| **A** | 0.0 (0.0) | 0.0 | 0.0 (0.0) | 0.0 |
| **(*E*)-B** | 34.5 (25.2) | 9.9 | −1.2 (−2.4) | −4.8 |
| **(*Z*)-B** | —[b](41.1) | 8.6 | −6.9 (−7.8) | −9.2 |
| **C** | 59.1 (47.4) | 17.7 | −5.3 (−2.4) | −2.8 |

[a] Total B3LYP/6–31G*–SCIPCM energies including ZPE corrections (in au) are −650.438330 (**7A**) and −631.037062 (**8A**). PM3–SCRF energies (kJ mol$^{-1}$) are −364.2 (**7A**) and −561.4 (**8A**).
[b] Not converged.

## RESULTS AND DISCUSSION

Before discussing the reactions of **7** and **8** with hydroxylamine, it is appropriate to address the possibility of a tautomeric equilibrium of both compounds [see Scheme 2 for the tautomerism of compound **8** as inferred from NMR spectroscopy;[7] since 3-acyltetronic and 3-acyltetramic acids and their six-membered analogues are known to be fully enolized[8,19] in the following only enol tautomers (**A–C**) are considered in detail]. According to NMR[7] spectroscopy for **8** the predominant (*ca* 80%) tautomeric form is the 3-hydroxyethylidene form (**Z**)-**8B** with an intramolecular hydrogen bond to the lactam oxygen atom. The 4-hydroxy form **8A** seems to be in a rapid equilibrium with the *E*-conformation **(E)-8B** of the hydroxyethylidene tautomer (*ca* 20%). Apparently no 2-hydroxy form **8C** is discernible in the NMR spectrum. In contrast, for **7** only one tautomeric species, the 3-acyl-4-methylamino form, is observable.[7] Results of B3LYP/6–31G*–SCIPCM and PM3–SCRF calculations for these tautomeric equilibria are summarized in Table 1.

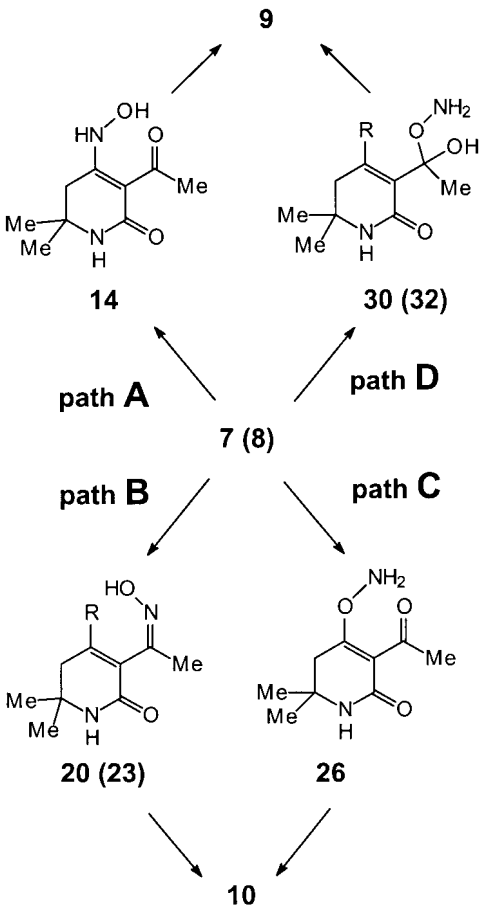


**Scheme 3**

In complete agreement with the experimental findings[7,8] and calculations on five-membered analogues,[19] for **7** the 3-acyl tautomer is predicted to be largely favored, especially at the B3LYP/6–31G* level of theory. In contrast, in the case of the 4-hydroxy compound **8** the hydroxyethylidene forms, especially that with an intramolecular hydrogen bond to the lactam carbonyl oxygen, should be the dominant species. However, in contrast to **7**, for compound **8** the preference for a single tautomer is less pronounced, also in agreement with the NMR results.[7]

Each of the two possible isoxazoles **9** and **10** can be obtained from either reactant **7** or **8** (independently of the respective tautomeric form) via two different paths (Scheme 3; in all following schemes compound numbers in parentheses refer to those with R = OH). Amine (or OH) exchange by addition of the hydroxylamine nitrogen (path A) at C-4 of **7** [**8A**; formation of oxime **35** (see Scheme 5) by addition to the C-4 carbonyl group in the case of tautomer **8B**] or, alternatively, reaction of the hydroxylamine oxygen at the acyl (hydroxyethylidene) carbon (path D) leads to compound **9**. Isoxazole **10** might be obtained by attack of the hydroxylamine nitrogen atom at the acyl (hydroxyethylidene) group [via oximes **20** and **23** or hydroxyaminoethylidene derivative **38** (see Scheme 7), respectively; path B] or its oxygen at C-4 (path C). In the following, results of the semi-empirical PM3 calculations on these four possible reaction pathways for both pyridinones **7** and **8** will be presented. For compound **8**, reactions of both tautomers **8A** and (**Z**)-**8B** are considered. Energies of the various transition states, intermediates, and products relative to the separated reactants **7** + **11** [**8A** + **11**, *(Z)*-**8B** + **11**; additional water or $H_3O^+$ molecules involved in (de)protonation steps as

**Table 2.** PM3 computed relative energies $E_{rel}$ (in kJ mol$^{-1}$) for the four paths A–D for compounds **7** and **8**[a]

| Path | **7** | $E_{rel}$ | **8A** | $E_{rel}$ | (**Z**)-**8B** | $E_{rel}$ |
|---|---|---|---|---|---|---|
| **Path A** | **7 + 11** | 0.0 | **8A + 11** | 0.0 | **8B + 11** | 0.0 |
| | **TS1** | 91.8 | **TS8** | 219.9 | **TS31** | 211.0 |
| | **12** | 69.4 | **18** | 157.3 | **34** | 8.2 |
| | **TS2** | 203.9 | **TS9** | 157.8 | **TS32** | 241.8 |
| | **13** | 71.3 | **14** | 8.5 | **35** | 13.6 |
| | **TS3** | 95.3 | **TS4** | 106.9 | **TS33** | 170.5 |
| | **14** | 18.5 | **15** | 30.2 | **36** | 131.8 |
| | **TS4** | 116.9 | **TS5** | 140.6 | **TS34** | 284.8 |
| | **15** | 40.2 | **16** | 9.5 | **9** | 42.1 |
| | **TS5** | 150.6 | **TS6** | 59.8 | | |
| | **16** | 19.5 | **17** | 1.8 | | |
| | **TS6** | 69.8 | **TS7** | 35.9 | | |
| | **17** | 11.8 | **9** | 32.9 | | |
| | **TS7** | 45.9 | | | | |
| | **9**[b] | −128.2 | | | | |
| **Path B** | **TS10** | 168.4 | **TS14** | 161.6 | **TS35** | 45.7 |
| | **19** | 9.2 | **22** | −0.7 | **37** | 25.3 |
| | **TS11** | 239.3 | **TS15** | 203.0 | **TS36** | 205.1 |
| | **20** | 11.3 | **23** | 19.1 | **38** | 13.4 |
| | **TS12** | 184.0 | **TS16** | 171.3 | **TS37** | 111.4 |
| | **21** | 148.0 | **24** | 135.6 | **39** | 37.3 |
| | **TS13** | 253.5 | **TS17** | 286.6 | **TS38** | 157.9 |
| | **10** | 50.7 | **10** | 40.7 | **40** | 20.0 |
| | | | | | **TS39** | 59.4 |
| | | | | | **29** | 10.0 |
| **Path C** | **TS18** | 265.3 | **TS24** | 278.7 | **TS40** | 242.9 |
| | **25** | 102.3 | **26** | 53.6 | **41** | 19.1 |
| | **TS19** | 146.1 | **TS20** | 233.1 | **TS41** | 94.7 |
| | **26** | 63.6 | **27** | 23.1 | **42** | 82.8 |
| | **TS20** | 243.1 | **TS21** | 31.6 | **TS42** | 264.2 |
| | **27** | 33.1 | **28** | 15.9 | **40** | 3.4 |
| | **TS21** | 41.6 | **TS22** | 24.6 | | |
| | **28** | 25.9 | **29** | 0.8 | | |
| | **TS22** | 34.6 | **TS23** | 49.0 | | |
| | **29** | 10.8 | **10** | 40.5 | | |
| | **TS23** | 59.0 | | | | |
| | **10**[b] | −120.5 | | | | |
| **Path D** | **TS25** | 212.2 | **TS28** | 261.7 | **TS43** | 279.7 |
| | **30** | 20.2 | **32** | 21.8 | **43** | 158.4 |
| | **TS26** | 123.3 | **TS29** | 103.8 | **TS44** | 164.2 |
| | **31** | 102.3 | **33** | 96.1 | **44** | 55.4 |
| | **TS27** | 211.2 | **TS30** | 255.8 | **TS45** | 230.0 |
| | **16** | 19.6 | **16** | 9.5 | **45** | 219.9 |
| | | | | | **TS46** | 255.3 |
| | | | | | **46** | 36.0 |
| | | | | | **TS47** | 86.4 |
| | | | | | **17** | 11.0 |

[a] $E_{rel}$ is given relative to the separated reactants **7** (**8**) + **11;** in the determination of $E_{rel}$ additional molecules ($H_2O$, $H_3O^+$, $MeNH_2$, $MeNH_3^+$) are included as required. PM3–SCRF heats of formation (kJ mol$^{-1}$) of the separated reactants are −364.2 (**7**), −561.4 (**8A**), −570.6 [(**Z**)-**8B**], −231.2 ($H_2O$), 389.9 ($H_3O^+$), −58.0 (**11**), −24.0 ($MeNH_2$), 425.9 $MeNH_3^+$).
[b] Protonation of $MeNH_2$ by $H_3O^+ \rightarrow MeNH_3^+ + H_2O$ included.

well as eliminated $MeNH_2(H_2O)$ (see Schemes 4–11) are included as required] for these reactions are summarized in Table 2.

## Path A

The reaction sequence computed by the PM3–SCRF method for the addition of the nitrogen atom of **11** to C-4 of **7 (8A)** is outlined in Scheme 4. For **7**, addition of **11** to C-4 (**TS1**), proton transfer to the methylamino group (**TS2**) and removal of the leaving group ($MeNH_2$, **TS3**) to **14** occurs in three distinct steps with well defined intermediates **12** and **13**. In contrast, replacement of the 4-hydroxy group in **8A** by $NH_2OH$ to **14** + $H_2O$ appears to be an almost concerted process, since elimination of $H_2O$ from the proton transferred intermediate **18** proceeds nearly barrierless (**TS9**).

 

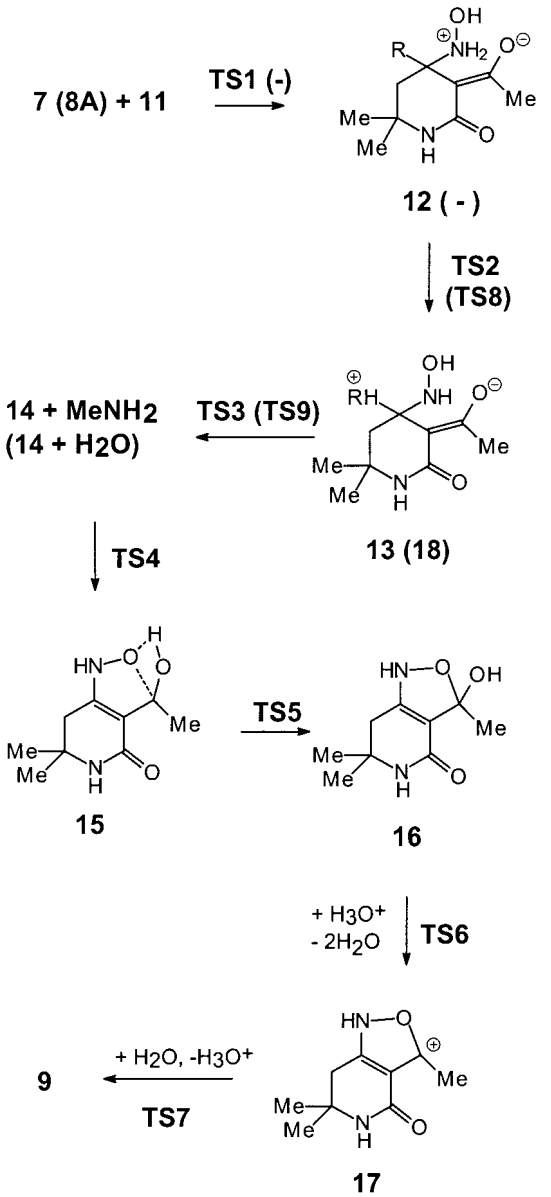


**Scheme 4**

The 4-hydroxyamino derivative **14**, obtained either from **7** or **8A**, then cyclizes (**TS4** and **TS5**) to intermediate **16**, which subsequently, by dehydration (**TS6**) and deprotonation (**TS7**), yields the final product **9**. Although both **7** and **8A** lead to the same common intermediate **14**, the relative energetics of the subsequent reaction steps (see Table 2) are different since the energies of the eliminated molecules $MeNH_2$ and $H_2O$, respectively, have to be taken into account. The rate-determining step in this reaction sequence is for both **7** and **8A** the addition of **11** to C-4 and, specifically, proton transfer to the substituent R (*i.e.* **TS2** and **TS8**, respectively). All subsequent steps are computed to have significantly lower activation energies. Furthermore, **7** is predicted to be more reactive than the hydroxy derivative **8A** [activation energy of 204 (**TS2**) *vs.* 220 kJ $mol^{-1}$ (**TS8**)].

Structural features of some representative transition states (**TS1** for addition/elimination, **TS2** for proton transfer, **TS5** for cyclization, **TS6** and **TS7** for dehydration and deprotonation, respectively) are presented in Fig. 1. The approach of the nucleophile to **7 (8A)** is facilitated by a hydrogen bond between the hydroxylamine OH and the 3-acyl group of **7 (8A)**. Development of the C-4—N-31 bond in **TS1** is accompanied by substantial pyramidalization at C-4. The height of this atom above the C-3—C-5—N-13 plane in **TS1** ($\Delta q$ = 24.5 pm) is approximately midway between the $sp^2$-hybridized C-4 of **7** ($\Delta q$ = 3 pm) and the tetrahedral intermediate **12** ($\Delta q$ = 43.1 pm). The rate-determining step, proton transfer between the two nitrogen atoms of the hydroxylamine and methylamino functionality (**TS2**), is characterized by a four-membered cyclic array of atoms perpendicular to the pyridinone moiety. The change in bonding distances in **TS2** appears to occur in an almost completely synchronous manner. In contrast, cyclization to **16** proceeds in an asynchronous, in fact two-step, fashion. Proton transfer from the 4-hydroxyamino group in **14** to the 3-acyl oxygen atom by far precedes ring closure (see **TS5** in Fig. 1). In **TS6** and **TS7** the expected[20] linear $[X\cdots H\cdots Y]^+$ arrangement is almost perfectly attained. The slight bend in **TS6** ($\angle$(O-10—H-11—O-12) = 161.5°) may be attributed to a deformation induced by hydrogen bonding between O-8 and H-14 (see Fig. 1).

Reaction of tautomer (***Z***)-**8B** via this pathway (Scheme 5) involves formation of the tetrahedral intermediate **34** and dehydration to oxime **35 (TS32)**. Subsequent cyclization **(TS33)** and dehydration **(TS34)** finally also leads to **9**. With respect to this pathway ***(Z)*-8B** should be even less reactive than tautomer **8A** [activation energy of 220 **(TS8)** *vs* 285 kJ $mol^{-1}$ **(TS34)**, see Table 2].

## Path B

As in path A, in this mechanism (see Schemes 6 and 7 for details) **11** reacts with its nitrogen end as a nucleophile. The first step in both **7** and **8A** involves a concerted addition at the acyl carbon and proton transfer to the carbonyl oxygen (**TS10** and **TS14** in Scheme 6) leading to the N,O-acetals **19** and **22**, respectively, followed by dehydration to oxime **20 (23)**. Subsequent cyclization, accompanied by elimination of the R group [**TS12 (TS16)** and **TS13 (TS17)**] finally yields the isoxazolo[4,5-*c*]pyridinone **10**. For both **7** and **8A**, cyclization of the oxime **20 (23)** via proton transfer from OH to MeNH (OH) (**TS13** and **TS17**, respectively) is calculated to have the highest energy relative to separated reactants [254 **(TS13)** and 287 **(TS17)** kJ $mol^{-1}$].

Reaction of tautomer ***(Z)*-8B** (see Scheme 7) proceeds in a similar manner with formation of the hydroxyaminoethylidene compound **38** instead of oxime **23** followed by a two-step cyclization to intermediate **40**. Dehydration of intermediate **40** leads to cation **29** common also to

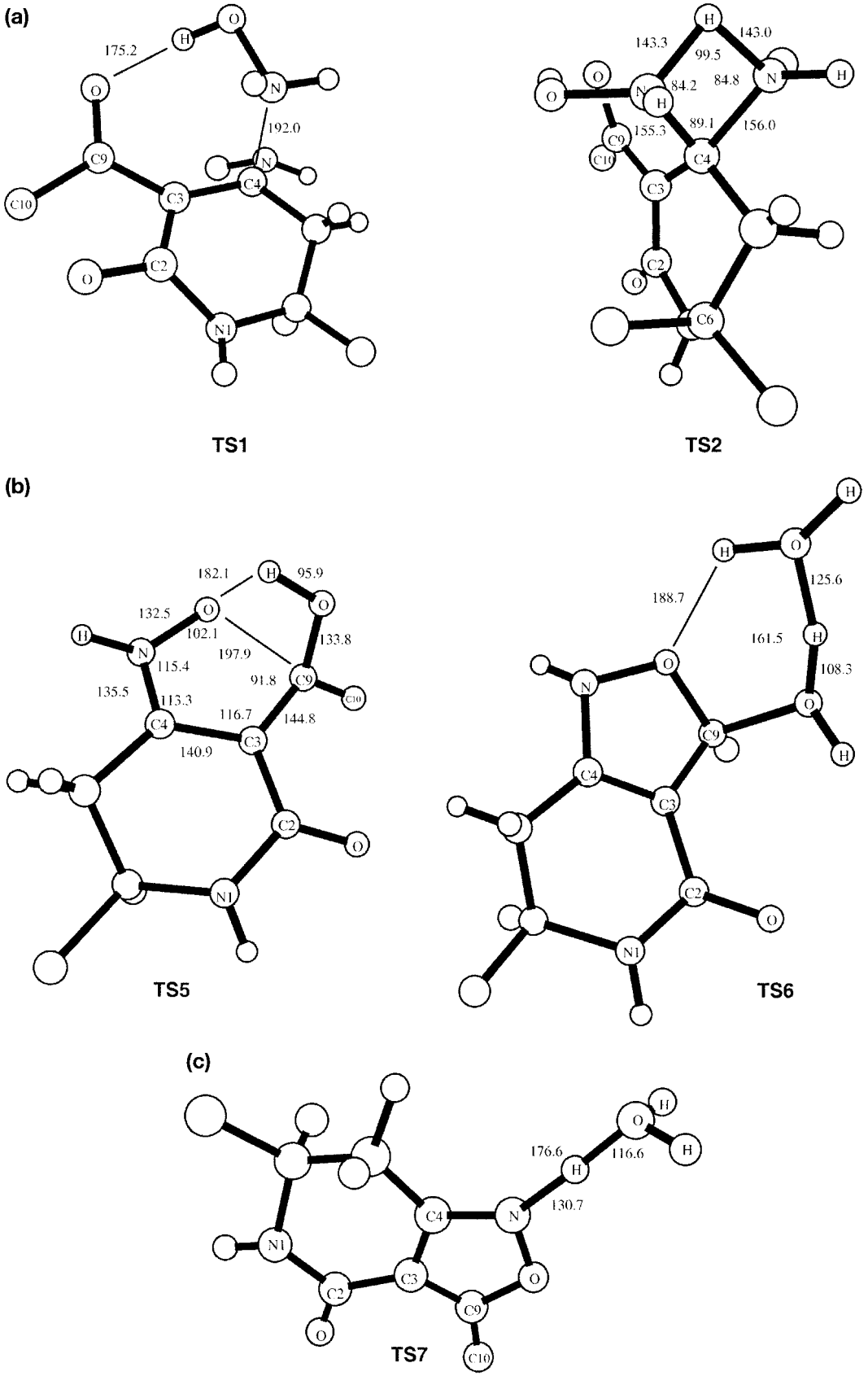


**Figure 1.** PM3–SCRF calculated structures of transition states **TS1, TS2, TS5, TS6** and **TS7**. Distances are given in pm and angles in degrees. Hydrogen atoms of methyl groups are omitted for clarity

 

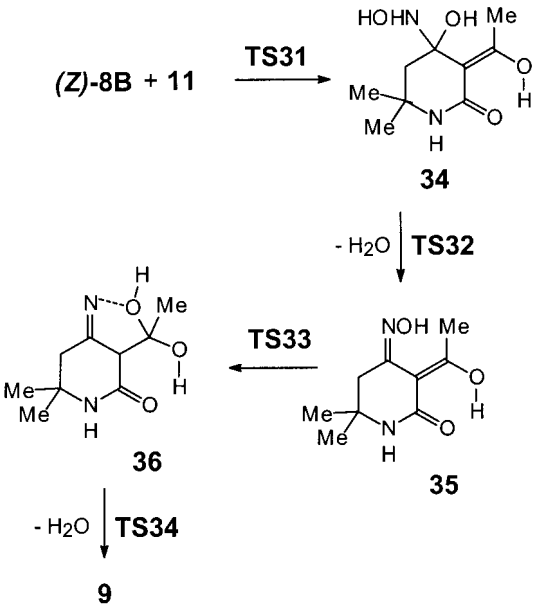


Scheme 5

reaction of both **7** and **8A** via path C (see Scheme 8 for further details).

Importantly, the activation energy for the formation of **10** by reaction of tautomer ***(Z)*-8B** is significantly lower (*ca* 80 kJ $mol^{-1}$) than for tautomer **8A**. Specifically, not only the first step, addition of the nucleophile to the exocyclic carbon atom (**TS14** *vs* **TS35**), is greatly favored in tautomer ***(Z)*-8B** but also cyclization of the intermediate **38 (TS38)** as compared with the reaction of

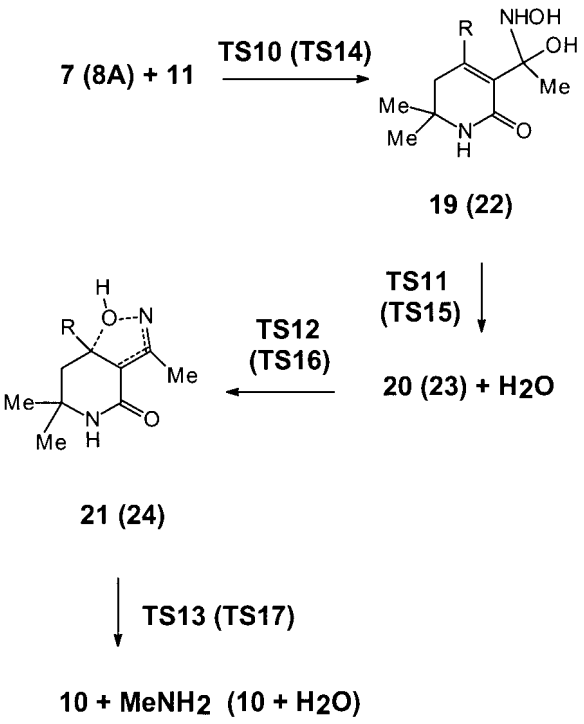


Scheme 6

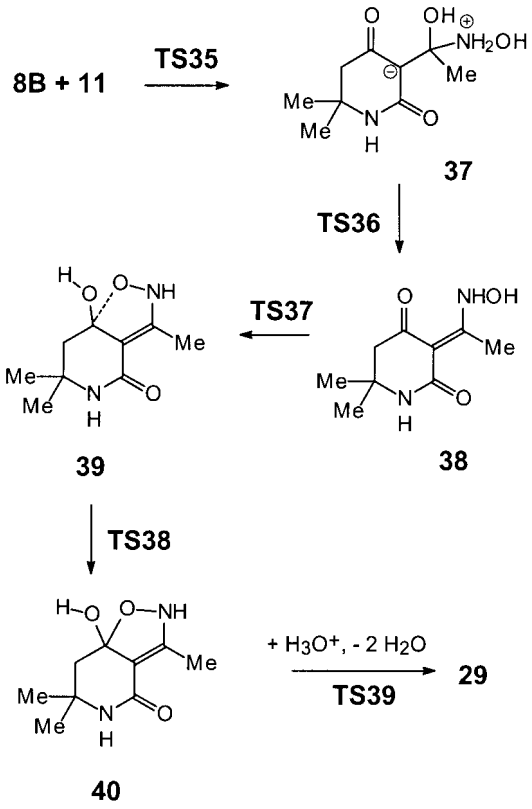


Scheme 7

oxime **23**. As opposed to reaction of **8A**, the rate-determining step is found to be formation of the hydroxyaminoethylidene intermediate **38 (TS36)** rather than its cyclization **(TS38)**. The structures of these two transition states are depicted in Fig. 2.

## Path C

The mechanistic details obtained by the PM3–SCRF calculations for hydroxylamine addition at C-4 of **7 (8)** via the oxygen atom of **11** are depicted in Schemes 8 and 9. Reaction of both starting compounds **7** and **8A** leads to the same common intermediate **26**. However, as already pointed out above, owing to different leaving groups ($MeNH_2$ and $H_2O$, respectively), the relative energies (see Table 2) are different. The overall features of this mechanism closely resemble those of path A. One difference is that here for **7** addition of **11** and proton transfer to the leaving group R [R=MeNH **(TS18)**] occurs in a concerted manner. Similarly to path A, for **8A** addition, proton transfer and elimination of R [R=OH **(TS24)**] are predicted to be essentially a one-step process. As found also for path A, the primary addition–proton transfer step **TS18 (TS24)** is rate determining. However, as indicated by the data presented in Table 2, formation of **10** involving reaction of the oxygen atom of **11** via path C appears to be highly unlikely. Computed

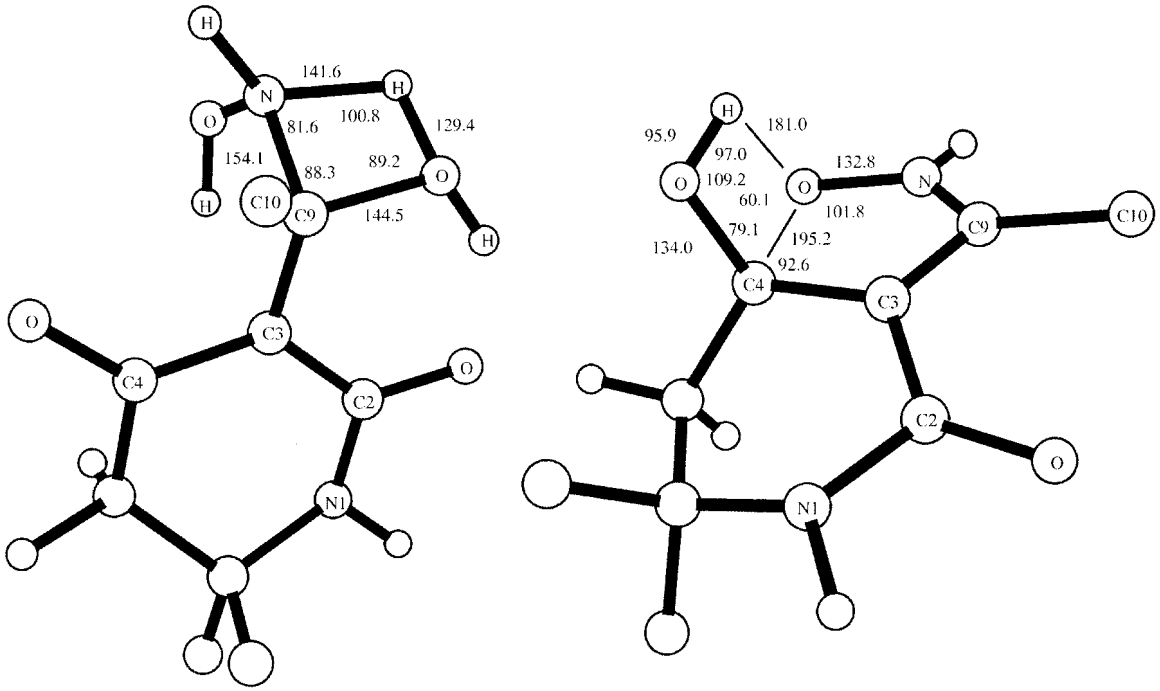


**Figure 2.** PM3–SCRF calculated structures of transition states **TS36** and **TS38**. Distances are given in pm and angles in degrees. Hydrogen atoms of methyl groups are omitted for clarity

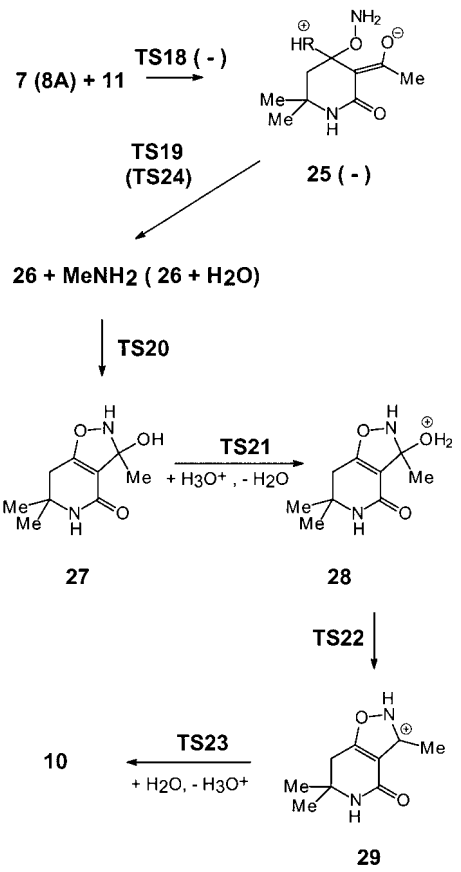


**Scheme 8**

activation energies for this alternative pathway are significantly higher, even more so for tautomer ***(Z)*-8B** (see Table 2 and Scheme 9), than those obtained for mechanism B.

## Path D

In the case of **7** and **8A**, the first step here is a concerted formation of the acetal **30 (32)** by addition–proton

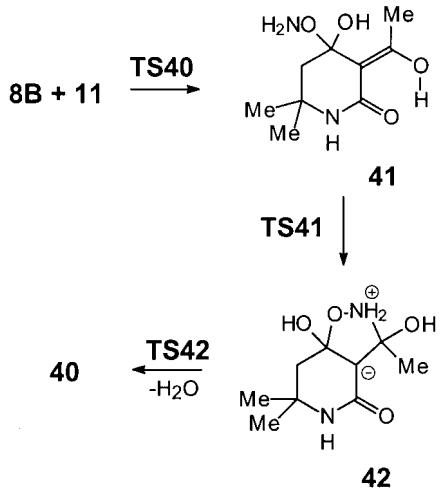


**Scheme 9**

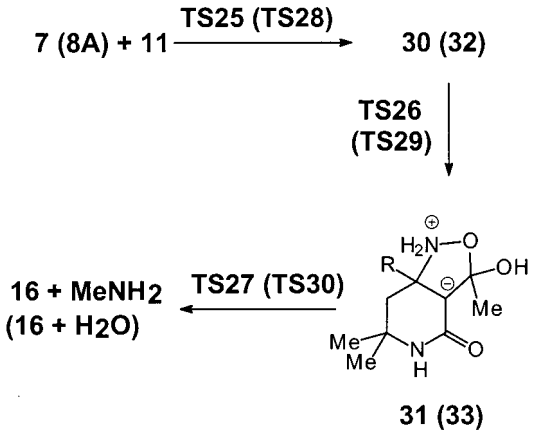


Scheme 10

transfer of the OH group of **11** to the 3-acyl group (see Scheme 10). Subsequent cyclization to intermediate **31 (33)** followed by proton transfer to R and elimination of $MeNH_2$ ($H_2O$) leads to intermediate **16** as also obtained in path A (see Scheme 4). Starting from this structure the reaction to **9** then proceeds as depicted in Scheme 4. Again, formation of the primary adduct **30 (32)** is rate determining. The calculated activation energies rule out this mechanism as a likely pathway for the formation of isoxazole **9**. For tautomer ***(Z)*-8B**, too, addition of **11 (TS43)** is rate determining (Scheme 11) with an even higher activation energy than that calculated for **TS28**.

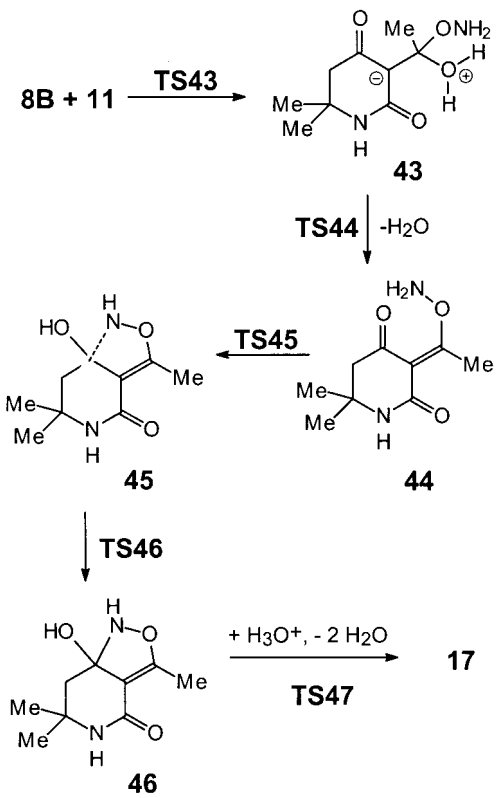


Scheme 11

Concerning the effect of the solvent on the calculated results, a comparison with those obtained for the gas phase (see Table 1 of the Supplementary Material) indicates that there is only little effect ($<10$ kJ mol$^{-1}$) for reactions involving only neutral molecules. However, there are substantial differences when charged particles are involved, especially for protonation/deprotonation steps. Inclusion of bulk solvent effects leads to a dramatic stabilization of $H_3O^+$ with a concomitant increase in activation energies in protonation steps. Neglecting the solvent results in unrealistically low or even negative activation energies for such processes.

Finally, it seems worthwhile to compare the present computational results with experimental investigations on related reactions.[21] Specifically, reaction of hydroxylamine **11** with $\beta$-keto esters preferentially occurs via attack of the nitrogen atom of **11** at the $\beta$-keto group. Under stopped-flow conditions,[22] the primary carbinol amine (corresponding to e.g. **19** or **34**) could be identified. Elimination of $H_2O$ to yield an oxime (corresponding to e.g. **20** or **35**) was found to be faster than cyclization. Ring closure of this oxime then yields isoxazolin-5-ones. This reaction sequence corresponds to formation of **9** from **8B** via path A or of **10** from **7 (8A)** via path B. Depending on the pH, formation of the isomeric isoxazolin-3-one is also observed.[21] It has been shown[21] that formation of this isomer occurs via $\beta$-keto hydroxamic acids rather than addition of the oxygen atom of **11** at the $\beta$-keto group. Since in the present molecules the ester functionality is lacking, such an alternative mechanism, if at all operative, must involve formation of an *O,O*-acetal by attack of the oxygen atom of **11**.

## CONCLUSION

From the data presented above, the following conclusions can be drawn. (i) Generally, the highest activation energies are found for the reaction of the nucleophile (N or O of $H_2NOH$) with the vinylic (C-4 or exocyclic) carbon atoms of compounds **7** and **8**. Thus, depending on the respective pathway, either addition of the nucleophile to the intermediate or its cyclization should be the rate-determining step. (ii) The highest barriers are obtained for TSs involving proton transfer. Solvent assistance is known to lower such barriers significantly; however, the unfavorable entropic contribution frequently offsets such an energy gain.[23] (iii) In agreement with chemical expectations, reaction of **11** involving its oxygen atom (paths C and D) are computed to be less feasible than those proceeding via the $NH_2$ group (paths A and B) as nucleophile. (iv) 4-Hydroxypyridinone **8A** is predicted to react via path B to oxime **23**. Using 3-acyl-4-hydroxyquinolones **3**, it has been found that amination exclusively occurs at the acyl functionality; no hydroxy exchange at C-4 could be detected.[5a,6] (v) The hydroxyethylidene tautomer (**Z**)-**8B** is not only more stable

than **8A** but also more reactive towards hydroxylamine. (vi) The propensity to react via path B to compound **10** is even more pronounced for tautomer **8B** than for **8A**. (vii) In striking contrast, in the reaction of compound **7** (R═MeNH) formation of isoxazolo[4,3-*c*]pyridinone **9** via path A should be favored over all other alternative reaction mechanisms. Such $\beta$-carbon additions accompanied by amine exchange indeed have been observed with compounds of type **7**.[24] The present computational results are also nicely corroborated by experimental findings on the related reaction of hydroxylamine with $\beta$-keto esters.[21,22] Based on the calculations, therefore, preferential formation of **9** and **10**, respectively, depending on whether 4-amino-**(7)** or 4-hydroxypyridinones (**8A** or **8B**) are used as starting materials, can be fully rationalized.

## REFERENCES


1. For a review on isoxazoles, see M. Sutharchanadevi and R. Murugan, in *Comprehensive Heterocyclic Chemistry II*, edited by A. R. Katritzky, C. W. Rees and E. F. V. Scriven Vol. **3**, pp. 221–260. Elsevier, Oxford (1996).
2. For a review on oxazoles, see F. W. Hartner, Jr, in *Comprehensive Heterocyclic Chemistry II*, edited by A. R. Katritzky, C. W. Rees and E. F. V. Scriven, Vol. **3**, pp. 261–318. Elsevier, Oxford (1996).
3. J. Nadelson, Sandoz, *US Pat*. 4 049 813 (1977); *Chem. Abstr.* **88**, 6862w (1978); J. Nadelson, Sandoz, *Ger. Offen.*, 2 609 127 (1976); *Chem. Abstr.* **85**, 192582r (1976); J. Nadelson, Sandoz, *US Pat*. 4 131 679 (1978); *Chem. Abstr.* **90**, 186802z (1979).
4. A. F. Khattab, *Liebigs Ann. Chem.* 393–395 (1996).
5. (a) P. Roschger and W. Stadlbauer, *Liebigs Ann. Chem.* 821–823 (1990); (b) P. Roschger and W. Stadlbauer, *Liebigs Ann. Chem.* 401–403 (1991); (c) W. Steinschifter, W. Fiala and W. Stadlbauer, *J. Heterocycl. Chem.* **31**, 1647–1652 (1994).
6. T. Kappe, R. Aigner, M. Jöbstl, P. Hohengassner and W. Stadlbauer, *Heterocycl. Commun.* **1**, 341–352 (1995).
7. R. Weis, K. Schweiger and W. M. F. Fabian, *Monatsh. Chem.* **129**, 1285–1292 (1998).
8. R. C. F. Jones, K. A. M. Duller and S. I. E. Vulto, *J. Chem. Soc., Perkin Trans. 1* 411–416 (1998).
9. J. Lessel, *Pharm. Acta Helv.* **71**, 109–119 (1996).
10. K. Bowden, R. J. Ranson, A. Perjéssy, M. Lácová, O. Hritzová and W. M. F. Fabian, *J. Phys. Org. Chem.* **11**, 467–474 (1998); K. Bowden, K. Agnihotri, R. J. Ranson, A. Perjéssy, P. Hrnciar, I. Prokeš and W. M. F. Fabian, *J. Phys. Org. Chem.* **10**, 841–848 (1997); K. Bowden, W. M. F. Fabian and G. Kollenz, *J. Chem. Soc., Perkin Trans. 2* 547–552 (1997); H. Stankovicová, W. M. F. Fabian and M. Lácová, *Molecules*, **1**, 223–235 (1996).
11. J. J. P. Stewart, *J. Comput. Chem.* **10**, 209–220, 221–264 (1989).
12. T. Clark, VAMP, Erlangen Vectorised Molecular Orbital Package, Version 4.40. Computer-Chemie-Centrum, University Erlangen-Nürnberg (1992).
13. J. Baker, *J. Comput. Chem.* **7**, 385–395 (1986).
14. (a) S. Miertuš, E. Scrocco and J. Tomasi, *Chem. Phys.* **55**, 117–129 (1981); (b) G. Rauhut, T. Clark and T. Steinke, *J. Am. Chem. Soc.* **115**, 9174–9181 (1993).
15. M. Orozco, C. Colominas and F. J. Luque, *Chem. Phys.* **209**, 19–29 (1993).
16. A. D. Becker, *J. Chem. Phys.* **98**, 5648–5652 (1993); C. Lee, W. Yang and R. G. Parr, *Phys. Rev. B* **37**, 785–789 (1988).
17. M. J. Frisch, G. W. Trucks, H. B. Schlegel, P. M. W. Gill, B. G. Johnson, M. A. Robb, J. R. Cheeseman, T. Keith, G. A. Petersson, J. A. Montgomery, K. Raghavachari, M. A. Al-Laham, V. G. Zakrzewski, J. V. Ortiz, J. B. Foresman, C. Y. Peng, P. Y. Ayala, W. Chen, M. W. Wong, J. L. Andres, E. S. Replogle, R. Gomperts, R. L. Martin, D. J. Fox, J. S. Binkley, D. J. Defrees, J. Baker, J. J. P. Stewart, M. Head-Gordon, C. Gonzalez, and J. A. Pople, Gaussian 94, Revision B.3. Gaussian, Pittsburgh, PA (1995).
18. K. B. Wiberg, H. Castejon and T. A. Keith, *J. Comput. Chem.* **17**, 185–190 (1996).
19. H. B. Broughton and P. R. Woodward, *J. Comput.-Aided Mol. Des.* **4**, 147–153 (1990).
20. Z. Latajka and S. Scheiner, *J. Mol. Struct.* **234**, 373–385 (1991); X. Duan and S. Scheiner, *J. Mol. Struct.* **270**, 173–185 (1992); X. Duan and S. Scheiner, *J. Am. Chem. Soc.* **114**, 5849–5856 (1992).
21. A. R. Katritzky, D. L. Ostercamp and T. I. Yousaf, *Tetrahedron* **43**, 5171–5186 (1987).
22. M. Cocivera, A. Effio, H. E. Chen and L. Vaish, *J. Am. Chem. Soc.* **98**, 7362–7366 (1976).
23. S. Antonczak, M. F. Ruiz-López and J.-L. Rivail, *J. Am. Chem. Soc.* **116**, 3912–3921 (1994); J. Pitarch, M. F. Ruiz-López, E. Silla, J.-L. Pascual-Ahuir and I. Tuñón, *J. Am. Chem. Soc.* **120**, 2146–2155 (1998); B. Kallies and R. Mitzner, *J. Mol. Model.* **4**, 183–196 (1998).
24. K. Schweiger and G. Zigeuner, *Monatsh. Chem.* **112**, 459–468 (1981); K. Schweiger, M. Schubert-Zsilavecz, R. Weis and F. Belaj, *Monatsh. Chem.* **123**, 133–143 (1992); H. Auer, R. Weis, K. Schweiger and M. Schubert-Zsilavecz, *Monatsh. Chem.* **125**, 571–577 (1994); H. Auer, R. Weis and K. Schweiger, *Monatsh. Chem.* **127**, 1027–1030 (1996).


 